VEGF modulates NMDA receptors activity in cerebellar granule cells through Src-family kinases before synapse formation

Claire Meissirel[a,b,1,2], Carmen Ruiz de Almodovar[c,d,1], Ellen Knevels[c,d,1], Cathy Coulon[c,d], Naura Chounlamountri[a,b], Inmaculada Segura[c,d], Pierre de Rossi[a,b], Stefan Vinckier[c,d], Kristof Anthonis[c,d], Bérangère Deléglise[a,b], Maria de Mol[c,d], Carine Ali[e,f,g], Karel Dassonville[a,b], Ellen Loyens[h], Jérôme Honnorat[a,b], Yvette Michotte[h], Véronique Rogemond[a,b], Ilse Smolders[h], Thomas Voets[i], Denis Vivien[e,f,g], Pieter Vanden Berghe[j], Ludo Van Den Bosch[d,k], Wim Robberecht[d,k,l], Alain Chédotal[m], Salvatore Oliviero[n], Mieke Dewerchin[c,d], Dietmar Schmucker[d,o], Nicole Thomasset[a,b,1], Paul Salin[a,b,p,1], and Peter Carmeliet[c,d,1,2]

[a]Institut National de la Santé et de la Recherche Médicale (INSERM), Unité 1028, Centre National de la Recherche Scientifique Unité Mixte de Recherche 5292, Neurooncology and Neuroinflammation, Lyon Neuroscience Research Center, F-69000 Lyon, France; [b]University Lyon 1, F-69000 Lyon, France; [c]Laboratory for Angiogenesis and Neurovascular Link, [k]Laboratory of Neurobiology, and [o]Laboratory of Neuronal Wiring, [d]Vesalius Research Center, VIB, K.U. Leuven, B-3000 Leuven, Belgium; [e]INSERM, Unité 919, Serine Proteases and Pathophysiology of the Neurovascular Unit, and [f]Centre National de la Recherche Scientifique, Unité Mixte de Recherche 6232, Center for Imaging Neurosciences and Applications to Pathologies, Cyceron, F-14074 Caen Cedex, France; [g]University of Caen Basse-Normandie, F-14074 Caen Cedex, France; [h]Department of Pharmaceutical Chemistry, Drug Analysis, and Drug Information, Vrije Universiteit Brussel, 1090 Brussels, Belgium; [i]Laboratory of Ion Channel Research, and [j]Center for Gastroenterological Research, Katholieke Universiteit Leuven, B-3000 Leuven, Belgium; [l]Department of Neurology, University Hospital Leuven, B-3000 Leuven, Belgium; [m]INSERM, Unité Mixte de Recherche S968, Department of Development, Institute of Vision, F-75012 Paris, France; [n]Department of Molecular Biology, Università di Siena, 53100 Siena, Italy; and [p]INSERM Unité 1028, Centre National de la Reserche Scientifique Unité Mixte de Reserche 5292, Physiopathology of the Sleep Neuronal Networks, Lyon Neuroscience Research Center, F-69000 Lyon, France

NMDA type glutamate receptors (NMDARs) are best known for their role in synaptogenesis and synaptic plasticity. Much less is known about their developmental role before neurons form synapses. We report here that VEGF, which promotes migration of granule cells (GCs) during postnatal cerebellar development, enhances NMDAR-mediated currents and Ca^{2+} influx in immature GCs before synapse formation. The VEGF receptor Flk1 forms a complex with the NMDAR subunits NR1 and NR2B. In response to VEGF, the number of Flk1/NR2B coclusters on the cell surface increases. Stimulation of Flk1 by VEGF activates Src-family kinases, which increases tyrosine phosphorylation of NR2B. Inhibition of Src-family kinases abolishes the VEGF-dependent NR2B phosphorylation and amplification of NMDAR-mediated currents and Ca^{2+} influx in GCs. These findings identify VEGF as a modulator of NMDARs before synapse formation and highlight a link between an activity-independent neurovascular guidance cue (VEGF) and an activity-regulated neurotransmitter receptor (NMDAR).

angiogenesis | neurovascular link | neuronal migration | cerebellum

VEGF and its receptor Flk1 (VEGFR-2) regulate several neurobiological processes in normal and pathological conditions (1). They stimulate neurogenesis, long-term potentiation, and learning, whereas low VEGF levels cause or aggravate motoneuron degeneration, and VEGF delivery delays paralysis in preclinical models (1). During cerebellar development, VEGF chemoattracts granule cells (GCs) from the external GC layer (EGL) toward the internal GC layer (IGL) (2). This chemotactic activity of VEGF for GCs in vivo is mediated by direct activation of Flk1 in GCs, independently of its angiogenic activity (2). However, the mechanisms via which VEGF regulates GC migration in the cerebellum remain unknown.

NMDA type glutamate receptors (NMDARs) are ligand-gated ion channels, permeable for Ca^{2+} (and other) ions that have been implicated in synaptic transmission and plasticity (3, 4), and may induce excitotoxity upon excessive activation (5). Interestingly, before neurons establish synapses, activation of NMDARs results in Ca^{2+} influx ($[Ca^{2+}]_i$), which promotes, among other processes, proliferation and survival of neuroblasts (6, 7), filopodia formation and growth cone turning (8, 9), and migration of cortical and cerebellar neurons (10–13). In general, NMDARs have been less extensively studied before synapse

formation than at developing or established synapses (14–16). It remains to be established whether NMDARs can be regulated by guidance cues during neuronal migration and, if so, the mechanism via which this process occurs has not been explored.

Prompted by findings that VEGF (1) and NMDARs (3, 17, 18) regulate neurogenesis, plasticity, and repair, we hypothesized that Flk1 activation might regulate NMDAR function. Because both NMDARs (NR1 and NR2B subunits) and Flk1 are expressed by migrating GCs (2, 19, 20) and regulate GC migration (2, 11–13), we explored a possible link between VEGF and NMDARs in GCs before synaptogenesis, when there are no excitatory glutamatergic synaptic inputs on GCs (21). Our findings identify VEGF as a modulator of NMDAR function in neurons before synapses are formed. We identify a unique interaction between receptors for a classic neurotransmitter and a prototypic angiogenic factor, which regulate neuronal migration in the developing cerebellum.

Results

VEGF Enhances NMDAR-Mediated $[Ca^{2+}]_i$ and Currents in GCs. To explore whether VEGF affects GC migration in part by modulating the NMDA response of migrating GCs, we examined by fura-2 fluorescence imaging whether activation of Flk1 by VEGF enhances $[Ca^{2+}]_i$ via NMDARs in GCs. Isolated GCs from postnatal day 5 (P5) mice, cultured for 1.0–1.5 d in vitro (DIV), express markers for EGL-like postmitotic GCs (22) but have not formed functional synapses yet (22, 23). Because VEGF can stimulate Ca^{2+} release from intracellular stores (24, 25) and $[Ca^{2+}]_i$ through

other channels than NMDARs (24, 26, 27), we selected a concentration of VEGF that, by itself, failed to elevate $[Ca^{2+}]_i$ in GCs. GCs were stimulated with a pulse of NMDA, exposed to vehicle or VEGF, and thereafter exposed again to NMDA. The increased $[Ca^{2+}]_i$ response to NMDA was comparable for the first and second pulse (Fig. S1A). However, when GCs were exposed to VEGF before the second NMDA pulse, the $[Ca^{2+}]_i$ response to the second pulse was increased compared with the first (Fig. 1 A and B), suggesting that VEGF enhanced NMDAR-mediated $[Ca^{2+}]_i$.
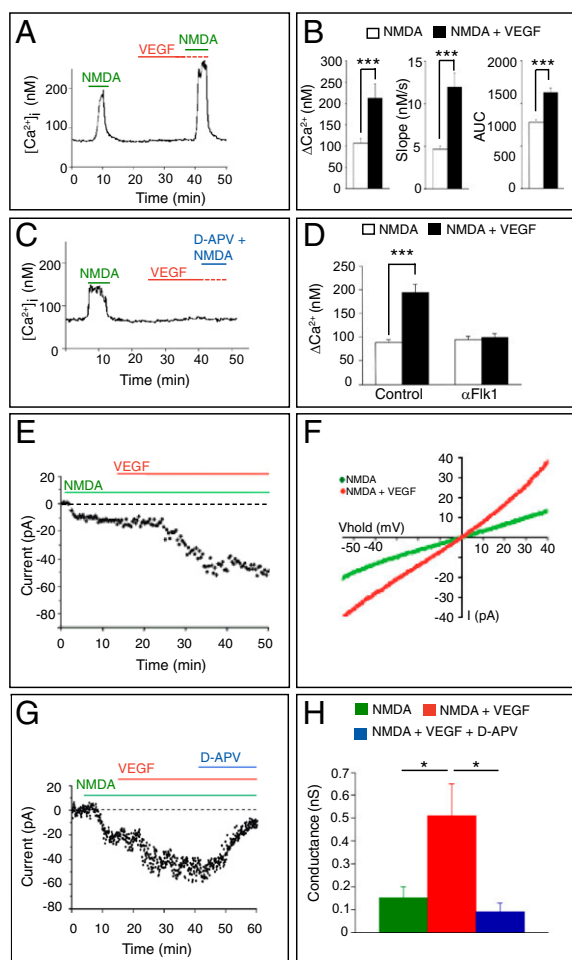

Fig. 1. VEGF enhances NMDA-stimulated $[Ca^{2+}]_i$ and NMDAR-mediated currents in GCs. (A) Representative single GC tracing of intracellular $[Ca^{2+}]_i$ levels obtained by Ca^{2+} imaging. GCs were stimulated with NMDA, exposed to control buffer or VEGF, and stimulated a second time with NMDA. VEGF amplified the second NMDA response. (B) Quantification of the VEGF-response. (Left) The difference between maximum $[Ca^{2+}]_i$ level and baseline $[Ca^{2+}]_i$ level (ΔCa^{2+}) was increased with VEGF ($n = 26$, ***$P < 0.001$). (Center) The maximal derivative of the rise in $[Ca^{2+}]_i$ levels (d$[Ca^{2+}]_i$/dt), the slope, was enhanced with VEGF ($n = 26$, ***$P < 0.001$). (Right) The area under the curve (AUC) was also increased with VEGF ($n = 26$, ***$P < 0.001$). (C) Single GC tracing of $[Ca^{2+}]_i$ showing blockage of $[Ca^{2+}]_i$ by D-APV. (D) Measurements of ΔCa^{2+} revealing inhibition of VEGF-dependent increase in $[Ca^{2+}]_i$ by αFlk1 but not by control IgG ($n = 44$, ***$P < 0.001$ for IgG; $n = 50$, $P =$ not significant for αFlk1). (E) Representative whole-cell patch–clamp recording of a GC in the lower EGL, revealing enhancement of the NMDA-induced current by VEGF. (F) Current–voltage relationship of the GC responses shown in E revealing increased inward currents in response to NMDA plus VEGF compared with NMDA alone ($n = 26$, ***$P < 0.001$). (G) Representative whole-cell patch-clamp recording showing that D-APV blocked the VEGF-enhancement of the NMDAR-mediated current. (H) NMDAR conductance was higher after VEGF plus NMDA than after NMDA alone; this conductance was blocked by D-APV ($n = 7$; *$P < 0.05$ in VEGF+NMDA vs. NMDA; *$P < 0.05$ in VEGF+NMDA vs. VEGF+NMDA+D-APV).

Control experiments showed that the NMDAR antagonist D-2-amino-5-phosphono-valerate (D-APV), added during the second NMDA pulse, abrogated the VEGF plus NMDA response (Fig. 1C), demonstrating that the VEGF effect is mediated via NMDARs. Incubation with an anti-Flk1 blocking antibody (αFlk1) (28), but not a control IgG, for 15 min before and during VEGF stimulation, blocked the VEGF-dependent increase in $[Ca^{2+}]_i$ (Fig. 1D and Fig. S1 B and C), revealing that binding of VEGF to its receptor Flk1 is required. αFlk1 did not alter NMDAR channel properties because it did not further reduce the NMDA signal (Fig. 1D and Fig. S1C). Similar findings were obtained when using the VEGF receptor tyrosine kinase inhibitor PTK787 (PTK) (Fig. S1D), showing that Flk1 signaling is required for the VEGF effect.

To further dissect the molecular characteristics of this VEGF-mediated effect on NMDAR, we reconstructed the cross-talk in cellulo by cotransfecting HEK-293 cells with NR1 and NR2B, with Flk1, or with the three together. When HEK-293 cells were cotransfected with only NR1 and NR2B, VEGF failed to potentiate the $[Ca^{2+}]_i$, indicating that VEGF did not directly affect NMDAR (Fig. S2A). Conversely, VEGF failed to increase $[Ca^{2+}]_i$ in cells transfected only with Flk1, indicating that VEGF did not induce a change in $[Ca^{2+}]_i$ by itself but required the presence of NMDARs (Fig. S2B). When all players were cotransfected, VEGF amplified the NMDA-induced $[Ca^{2+}]_i$ (Fig. S2C). Without VEGF, the second pulse of NMDA did not increase $[Ca^{2+}]_i$ above the level induced by the first pulse (Fig. S2D). Thus, VEGF potentiates NMDAR-mediated $[Ca^{2+}]_i$ in GCs before synapse formation and in cotransfected HEK-293 cells via Flk1 signaling.

We also confirmed that the VEGF-dependent enhancement of NMDAR activity was operational in GCs in situ. In the cerebellum, Flk1 is present in migrating GCs, whereas Flt1/VEGFR-1 is not detectable (2). We used whole-cell patch–clamp techniques in acute cerebellar slices of P9–P10 mice to record NMDA-evoked currents in GCs in the lower layer of the EGL, before synapse formation (21). Because no synaptic events were recorded in GCs from the lower EGL (Fig. S3 A and B), consistent with the absence of synaptic input in migrating GCs (21), we superfused NMDA and its receptor antagonist D-APV and applied VEGF topically to minimize possible indirect effects. Application of VEGF alone induced only a small inward current (Fig. S3 C–E). Consistent with previous reports (20, 29), NMDA evoked an inward current in GCs in the lower EGL (Fig. 1 E–H). Notably, VEGF enhanced the NMDA-induced current already within 10–15 min by more than twofold (Fig. 1 E–H). This VEGF-induced potentiation was observed when NMDA was used at 50 μM or lower concentrations (Fig. S4A) and was blocked by D-APV (Fig. 1 G and H), indicating that the VEGF response in GCs is mediated through NMDARs.

To evaluate whether the effect of VEGF on NMDAR is mediated by Flk1 signaling, we silenced Flk1 in GCs by ex vivo electroporation (2). We generated a shRNA construct to silence Flk1 (Flk1^{KD}) and used a scramble as control (Flk1^{Ctl}). Validation experiments showed detectable Flk1 protein levels in HEK-293 cells transfected with a Flk1-expression plasmid and Flk1^{Ctl} (Fig. S4B). In contrast, cotransfection with Flk1-expression plasmid and Flk1^{KD} abolished Flk1 expression (Fig. S4B), indicating silencing by Flk1^{KD}. These constructs were coelectroporated with an EGFP expression vector in cerebella ex vivo, and cerebellar slices were cultured as described (2). After 3 d in culture, whole-cell patch–clamp recordings of GFP$^+$ GCs in the lower EGL showed that Flk1 silencing abrogated the VEGF-induced potentiation of NMDAR-mediated currents (Fig. S4C). Thus, the VEGF-evoked increase in $[Ca^{2+}]_i$ and currents in GCs require Flk1 and are mediated via NMDARs before synapse formation.

Flk1 Interacts with NMDARs. Prompted by the link between VEGF and NMDAR, we assessed whether Flk1 associates with NMDARs in GCs. During cerebellar development, Flk1 and NR2B are expressed in migrating GCs and are needed for GC migration (2, 12, 13). Both molecules were found to be coexpressed by GCs

when migrating along Bergmann glia fibers in vitro (Fig. 2A). We therefore focused on NR2B. We immunoprecipitated Flk1 from GCs, or from cotransfected HEK-293 cells, and immunoblotted these precipitates with anti-NR1 or anti-NR2B antibodies. NMDAR subunits coimmunoprecipitated with Flk1 in both cell types, whereas a control antibody was ineffective (Fig. 2 B and C). Similar results were obtained when anti-NR2B was used for immunoprecipitation and anti-Flk1 was used for immunoblotting (data not shown), indicating that Flk1 and NR1/NR2B associate with each other.

We next investigated whether Flk1 and NMDARs cluster together on the cell surface of GCs, before forming synapses. Because VEGF enhanced NMDAR-mediated $[Ca^{2+}]_i$ and currents in GCs within 10–15 min after application, we stimulated GCs (1 DIV) for 10 min with VEGF and stained nonpermeabilized GCs for Flk1 and NR2B. High-resolution imaging was used to determine receptor clusters by using established methods (14) (Fig. S5 A–H). In baseline, Flk1 was present on the cell surface but only a few Flk1 clusters were formed, NR2B clusters were readily detected, and only a few Flk1/NR2B coclusters were present (Fig. 2D). Notably, VEGF increased the number of Flk1 clusters and Flk1/NR2B coclusters, without affecting the number of NR2B clusters (Fig. 2D). Exposure of GC growth cones to VEGF-soaked heparin beads also increased the surface expression of NR2B and Flk1 (Fig. S5 I and J). Thus, Flk1 interacts with NR1 and NR2B, and VEGF increases the number of Flk1/NR2B coclusters on the GC surface.

Flk1 Activation by VEGF Enhances NR2B Phosphorylation via Src-Family Kinases (SFKs). Phosphorylation of NMDARs by SFKs increases NMDAR-mediated currents and $[Ca^{2+}]_i$ (30, 31). SFKs phosphorylate tyrosine residues in the intracellular tail of NR2B, leading to a greater number of active NMDAR channels at the cell surface (32, 33). We thus examined whether the amplification of the NMDAR-dependent $[Ca^{2+}]_i$ by VEGF/Flk1 in GCs relied on

an increase in NR2B tyrosine phosphorylation by SFKs. VEGF activated SFKs in GCs, as revealed by the increased SFK-Tyr[416] phosphorylation (Fig. 3A). To explore whether VEGF also stimulates phosphorylation of NR2B, GCs lysates were immunoprecipitated with an antibody for phosphorylated tyrosine (pTyr), and precipitates were immunoblotted for NR2B. As shown in Fig. 3B, VEGF increased NR2B tyrosine phosphorylation in GCs.

To facilitate further molecular mapping of this pathway, we used cotransfected HEK-293 cells because this cellular model exhibits the same VEGF-induced effect on NMDARs as GCs (as described above). As expected, VEGF activated Flk1 signaling, revealed by increased phosphorylation of Flk1-Tyr[1173] (Fig. 3C). VEGF also increased the phosphorylation of Flk1-Tyr[949], acting as a docking site for SFKs (34, 35) (Fig. 3C). Immunoblotting for αSrc-pTyr[416] showed that VEGF activated SFKs (Fig. 3D and Fig. S6B). Finally, VEGF also increased tyrosine phosphorylation of NR2B (Fig. 3E). This phenomenon was also observed when VEGF was used in combination with NMDA (Fig. S6A).

We next analyzed whether the increase in NR2B phosphorylation by VEGF relied on SFKs. We therefore coexpressed NR1, NR2B, and Flk1 together with an active form of Src (Src[WT]) or a dominant-negative mutant form of Src (Src[DN]) in which the kinase domain was inactivated (K295R) and the regulatory domain was mutated (Y527F); this dominant-negative Src[DN] is well known to block SFKs (36, 37). Src[DN] abrogated the increase in NR2B tyrosine phosphorylation by VEGF (Fig. 3F and Fig. S6 A and B). We also used a NR2B mutant (NR2BTM) in which the tyrosine residues that become phosphorylated by SFKs are mutated to phenylalanines and are no longer phosphorylated (15). Coexpression of Flk1, NR1, and NR2BTM abolished VEGF-induced NR2B phosphorylation (Fig. 3G). Thus, activation of Flk1 by VEGF stimulated SFK-dependent tyrosine phosphorylation of NR2B.

VEGF Enhances NMDAR-Mediated $[Ca^{2+}]_i$ and Currents via SFKs. To link the VEGF-induced phosphorylation of NR2B to the increased NMDAR-mediated $[Ca^{2+}]_i$ by VEGF, we measured the $[Ca^{2+}]_i$ in HEK-293 cells cotransfected with Flk1, NR1, and either NR2B or NR2BTM. Compared with controls, cells expressing NR2BTM did not exhibit the VEGF-dependent amplification of the NMDA-induced $[Ca^{2+}]_i$ (Fig. 3H). Furthermore, to demonstrate an involvement of SFKs, we blocked the SFK activity in electrophysiological measurements directly in the recorded GCs by administering the SFK inhibitor PP1 via the patch pipette using previously described methods (38). SFK blockade abolished the amplification of the NMDAR-mediated currents by VEGF in GCs, whereas the inactive homolog PP3 was ineffective (Fig. 3I and Fig. S7 A and B). Calcium imaging studies in GCs confirmed that PP1, but not PP3, abrogated the potentiation by VEGF of the $[Ca^{2+}]_i$ transients in response to NMDA (Fig. 3J and Fig. S7 C and D). Thus, VEGF-dependent activation of SFKs enhances NMDAR currents and $[Ca^{2+}]_i$ via tyrosine phosphorylation of NR2B.

VEGF Promotes GC Migration via NMDAR Activation. We recently reported that VEGF attracts GCs during cerebellar development (2). To explore the physiological relevance of the VEGF/NMDAR link in this process, we used a modified Boyden chamber assay (39) and counted GCs migrating to the lower side of the filter. When VEGF was added to the lower compartment, GC migration was enhanced, indicating that VEGF is chemotactic for GCs (Fig. 4A and Fig. S8A). Addition of D-APV to the upper chamber did not affect GC motility, suggesting that endogenous glutamate, released by GCs (40), could not activate NMDAR in these conditions (Fig. 4A). However, when added together with VEGF, D-APV reduced the chemotactic GC response to VEGF (Fig. 4A), implying that the effect of VEGF relies on NMDAR activation. These data suggest a model whereby VEGF sensitized NMDAR to the low levels of endogenous glutamate and thereby stimulated GC migration.

To further underscore the relevance of the VEGF/NMDAR link for GC migration in a more in vivo-like microenvironment,
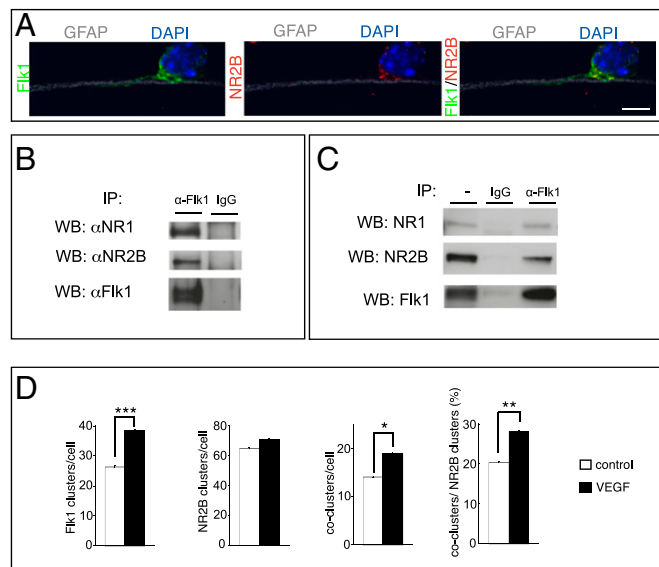

Fig. 2. Flk1 associates with NR1 and NR2B. (A) Confocal image of a GC migrating along a glia fiber (GFAP+; gray/white), showing Flk1 (green) and NR2B (red) expression at the plasma membrane; counterstaining is DAPI (blue). (B and C) Lysates of GCs (B) or cotransfected HEK-293 cells (C) were immunoprecipitated with an anti-Flk1 antibody (α-Flk1) or with a control IgG and immunoblotted for NR1 (top lane), NR2B (middle lane), or Flk1 (bottom lane). (D) Quantification of Flk1 or NR2B clusters and of Flk1/NR2B coclusters at the GC surface, revealing that VEGF stimulation did not affect the number of NR2B clusters (n = 54–46, P = not significant) but increased the number of Flk1 clusters (n = 54–46, ***P < 0.001) and Flk1/NR2B coclusters (n = 54–46, *P < 0.05 for coclusters per cell; **P = 0.005 for percentage of coclusters/NR2B clusters). (Scale bar: A, 5 μm.)

Fig. 3. VEGF-dependent SFK activation induces NR2B tyrosine phosphorylation and potentiation of NMDAR activity. (*A*) Immunoblot of GC lysates using antibodies against SFK-pTyr^{416} (αSrc-pTyr^{416}) or total Src (αSrc) showing increased activation of SFKs after VEGF stimulation. (*B*) GC lysates were immunoprecipitated with an anti-pTyr antibody and immunoblotted for NR2B, showing increased NR2B phosphorylation upon VEGF stimulation. Bottom lane shows the NR2B immunoblot of total cell lysates. (*C*) Lysates of cotransfected HEK-293 cells immunoblotted for Flk1-pTyr^{1173} or Flk1-pTyr^{949} (top and middle lanes) or total Flk1 (bottom lane), showing that VEGF activated Flk1. (*D*) Lysates of cotransfected HEK-293 cells were immunoblotted for pTyr^{416}-SFK or total Src, showing that VEGF activated SFKs. (*E*) Lysates of cotransfected HEK-293 cells were immunoprecipitated with an anti-pTyr antibody and immunoblotted for NR2B, showing that VEGF induced NR2B phosphorylation (upper lane). Immunoblotting of cell lysates showed comparable expression of NR2B (lower lane). (*F*) Lysates of HEK-293 cells, cotransfected with WT Src (Src^{WT}) or dominant-negative Src (Src^{DN}) together with NR1, NR2B, and Flk1, were immunoprecipitated with an anti-pTyr antibody and immunoblotted for NR2B, showing increased NR2B phosphorylation in Src^{WT} but not in Src^{DN} cells (top lane). Immunoblotting of cell lysates showed comparable expression of NR2B (middle lane) and increased levels of Flk1-pTyr^{1173} in response to VEGF (bottom lane). (*G*) Lysates of HEK-293 cells cotransfected with NR2BTM, NR1, and Flk1 were immunoprecipitated with an anti-pTyr antibody and immunoblotted for NR2B, showing that VEGF did not increase phosphorylation of NR2BTM (top lane). Immunoblotting of cell lysates showed comparable expression of NR2BTM (middle lane) and increased levels of Flk1-pTyr^{1173} in response to VEGF (bottom lane). (*H*) The increase in NMDAR-stimulated [Ca^{2+}]$_i$ (ΔCa^{2+}) was observed in HEK-293 cells cotransfected with Flk1, NR1, and NR2B ($n = 21$, ***$P < 0.001$) but not with Flk1, NR1, and NR2BTM ($n = 44$, $P =$ not significant). (*I*) The increase in NMDAR whole-cell patch-clamp conductance by VEGF was inhibited by PP1 ($n = 7$, $P =$ not significant) but not by PP3 ($n = 7$, **$P < 0.01$). (*J*) The increase of the NMDA-induced ΔCa^{2+} by VEGF was blocked by PP1 ($n = 36$, $P =$ not significant) but not by PP3 ($n = 50$, ***$P < 0.001$).
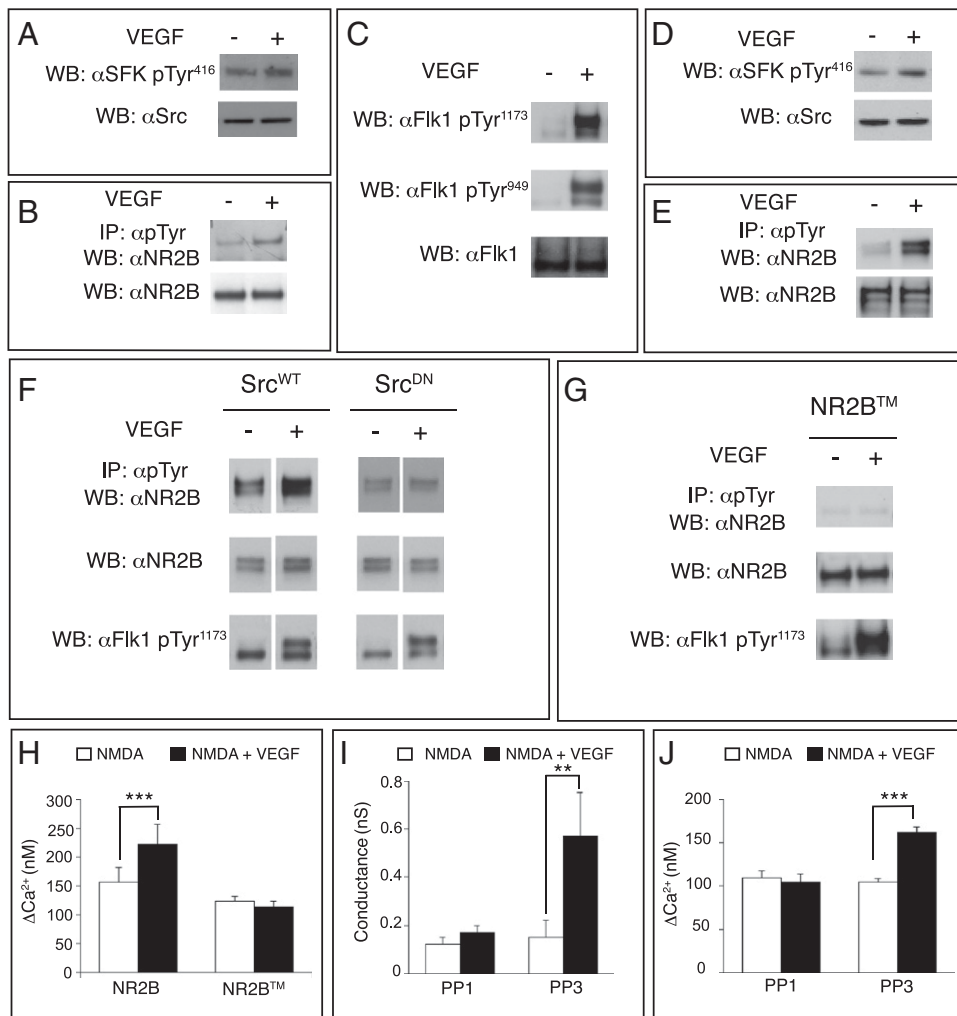
we used organotypic cerebellar slices (39). Migrating GCs were traced by labeling proliferating GCs with a BrdU pulse in vivo at P10, 3 h before we dissected the cerebella and cultured the slices. Treatment with αFlk1 reduced GC migration, showing that endogenous VEGF regulated GC migration (Fig. 4*B*), as reported in our in vivo findings (2). Consistent with previous results (11), treatment of slices with D-APV inhibited GC migration (Fig. 4*B* and Fig. S8*C*), indicating that endogenous glutamate activates NMDARs in these conditions. To explore whether endogenous VEGF sensitized NMDARs to endogenous glutamate, we treated slices with αFlk1 and D-APV together. We reasoned that, if VEGF would regulate GC migration independently of NMDAR, blockage of Flk1 plus NMDAR should induce a greater effect than single blockage of each molecule alone. If, however, VEGF would regulate GC migration by enhancing NMDAR activity through a Flk1/NMDAR modulation, then one would expect not only that αFlk1 and D-APV should induce a comparable antimigratory effect (Fig. 4*B*) but also that combined blockage of Flk1 and NMDAR should not induce a greater effect than single blockage of either molecule alone. In support of the latter mechanism, αFlk1 plus D-APV did indeed not reduce GC migration more than each compound alone (Fig. 4*B*). Similar results were obtained when GC migration was analyzed in

organotypic slices from cerebella electroporated with shRNA constructs for Flk1 (Flk1^{KD}) and treated with D-APV (Fig. S8*C*).

Discussion

In this study, we identified VEGF as a modulator of NMDAR function before synapse formation and documented a unique link between a receptor for a classic neurotransmitter (NMDAR) and a receptor for an angiogenic factor and a neuronal guidance cue (Flk1), both of which are needed for proper GC migration in the developing cerebellum. A combination of electrophysiological, biochemical, Ca^{2+} imaging, and other cell-biological studies in primary GCs and transfected HEK-293 cells revealed that Flk1 associates with NR1 and NR2B in a complex, that Flk1 and NMDARs form increased numbers of coclusters in GCs upon VEGF stimulation, and that VEGF increases NMDAR-mediated currents and [Ca^{2+}]$_i$. The rapidity of the VEGF-mediated amplification of the NMDAR activity (within minutes) suggests that this modulation relies on posttranslational mechanisms. Indeed, VEGF stimulated NMDARs via SFK-dependent phosphorylation of tyrosine residues in the cytosolic domain of NR2B. Overall, these results identify a molecular framework whereby binding of VEGF to Flk1 activates SFKs, leading to NR2B
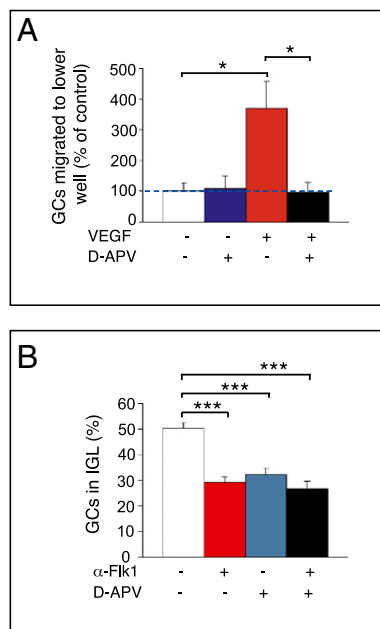
NEUROSCIENCE

Fig. 4. VEGF-induced potentiation of NMDAR activity promotes GC migration. (*A*) Quantification of GC migration in Boyden chamber assay, showing that supplementation of D-APV (10 μM) to the upper chamber (blue bar) does not affect GC motility compared with the control condition (white bar). When VEGF (50 ng/mL) is added to the lower chamber (red bar), GC migration is increased. This increase is inhibited by adding D-APV (10 μM) in the upper chamber (black bar, *$P < 0.05$). (*B*) Analysis of GC migration in organotypic cerebellar slices [expressed as percentage of BrdU⁺ GCs in the IGL versus total number of BrdU⁺ GCs in EGL, molecular layer (ML), and IGL], showing inhibition of GC migration upon αFlk1 treatment (red bar) and upon D-APV treatment (blue bar). The combination of αFlk1 and D-APV does not reduce GC migration further (black bar; ***$P < 0.001$).

phosphorylation and enhancement of NMDAR-mediated currents and $[Ca^{2+}]_i$.

The molecular pathways via which VEGF promotes neuronal migration and neurite outgrowth are largely unknown, in contrast to the wealth of information about the molecular signaling mechanisms of VEGF/Flk1 in endothelial cells (34). In these cells, binding of VEGF to Flk1 stimulates migration and vascular permeability in part via activation of SFKs (41). Our studies in GCs now show that VEGF also activates SFKs in these neurons and that SFKs transmit intermediary signals from Flk1 to NMDAR to enhance the conductance and $[Ca^{2+}]_i$ of NMDAR channels. SFKs regulate NMDARs in part by preventing internalization of activated surface-exposed NMDARs as well as by regulating ion channel properties (32). In GCs in the absence of synapses, we also observed that VEGF increased the formation of cell surface Flk1/NR2B coclusters.

During postnatal cerebellar development, migrating GCs predominantly express the NR2B subunit (19), and, when blocked, GC migration is impaired (12). Further evidence that NMDARs regulate GC migration is provided by findings that GC migration is inhibited by NMDAR blockade and accelerated by enhanced NMDAR activity (11, 13). In a recent study, we documented that VEGF controls GC migration as a chemotactic guidance cue in the developing cerebellum in vivo (2). Using the Boyden chamber assay in vitro and the organotypic cerebellar slice model ex vivo, we now show that VEGF is chemotactic for GCs in a NMDAR-dependent manner. Because elevated Ca^{2+} levels in response to NMDAR activation promote filopodia formation, turning responses, and neuronal motility (8, 11, 42), amplification of NMDARs activity by VEGF would enhance neuronal migration. Because VEGF is present as a gradient in the developing cerebellum (2), sensitization of NMDARs by

VEGF to glutamate may explain why migrating GCs become progressively chemoattracted to the highest levels of VEGF in the deeper layers of the cerebellar cortex. The finding that activation of Flk1 and NMDAR together also stimulates chemokinesis (Fig. S8*B*) may further explain how VEGF regulates GC migration. Overall, this study provides unique molecular mechanistic insights in how VEGF regulates neuronal migration.

Previous studies documented that ephrin-b2 and neuregulin enhance the activity of NMDARs through SFK-dependent phosphorylation of particular NR2 subunits (15, 43). In contrast to our study, however, those reports documented regulation of synaptic NMDAR at the postsynaptic site and reported how these molecules amplified the activity of NMDAR in synaptogenesis, synaptic transmission, and plasticity. We show here that VEGF modulates the NMDAR activity during migration of immature GCs before they form synapses. Intriguingly, however, the VEGF/NMDAR link may not be restricted alone to NMDARs before synapse formation and be even of broader (patho)physiological relevance because hippocampal and motor neurons, known to express synaptic NMDARs (NMDARs), also express Flk1 (44, 45).

Overall, the role for VEGF as a modulator of NMDAR activity provides further evidence for the importance of the neurovascular link. Given the expression of VEGF and Flk1 in many cell types in the central nervous system (1, 46) as well as the general implication of NMDARs in numerous neurobiological processes in health and disease, these findings also raise intriguing questions about the possible role of this identified VEGF/NMDAR link in nondevelopmental processes, including learning, memory, synaptic plasticity, and neurodegeneration. It will be also necessary to further dissect the molecular details of how VEGF precisely influences the activity of NMDARs in providing neuroprotection versus excitotoxicity (47). Furthermore, defects in stimulating NMDAR phosphorylation by neuregulin has been implicated in the pathogenesis of schizophrenia (46, 48). More speculatively, it will be therefore interesting to examine whether defective stimulation of NMDAR phosphorylation by insufficient VEGF might also increase the susceptibility of neurons to dysfunction or degeneration. As for now, our findings of how an activity-independent signal (VEGF) regulates a receptor for a classic neurotransmitter provide a unique insight into the molecular basis of brain wiring.

Materials and Methods

GC Purification and Chemotaxis Assay. GCs were purified as described in ref. 49.

Immunohistochemistry. Purified GCs were fixed in nonpermeable conditions and stained with antibodies recognizing extracellular epitopes of the corresponding proteins. Cerebellar slices were fixed for 2 h in 4% PFA at room temperature and subsequently processed for BrdU immunostaining.

Analysis of Flk1 and NR2B Coclusters. Analysis of Flk1 and NR2B coclusters was performed by using the image analysis software package Imaris (version 6.3.1) (Fig. S5). Clusters were detected in the maximum projection of 3D confocal z-stack images.

Electrophysiological Recordings. Whole-cell patch–clamp recordings were performed on acute parasagittal cerebellar slices (200–300 μm thick) (2, 50) from P8 C57BL6 mice. GCs were characterized electrophysiologically by their absence of action potentials and synaptic events and by their high input resistance and small cell capacitance (29). NMDA (50 μM; Tocris) was added to the perfusion solution, and VEGF (150 ng/mL; R&D Systems) was topically applied by pressure (Picospritzer II). NMDAR-mediated responses were blocked with D-APV (50 μM; Tocris).

Ex Vivo Cerebellar Electroporation. Cerebella dissected from P8 or P10 mice were electroporated as previously described (2). See SI Materials and Methods for details of the used shRNAi constructs.

Transfection of HEK-293 Cells. The following plasmids were used for transfection: Flk1, NR1, NR2B-GFP (termed NR2B), NR2BTM, Src^WT, Src^DN, shFlk1^KD, and shFlk1^Ctl. For the phosphorylation experiments, cells were starved 1 d after transfection in 0.1% serum containing medium for 16–20 h.

Calcium Imaging. Cell cultures of primary GCs (1–1.5 DIV) or transfected HEK-293 cells were loaded with 5 μM fura-2-acetoxymethyl ester plus 0.1% Pluronic F-127 (Molecular Probes) and incubated for 60 min in Hepes-buffered saline solution (HBSS). NMDA pulses and washes were performed with a perfusion system, and the rest of the incubations and treatments were performed without perfusion.

Immunoprecipitation and Immunoblotting. GCs or transfected HEK-293 cells were stimulated with VEGF (50 ng/mL) for 15 or 5 min, respectively, and lysed afterward. For immunoprecipitation, 400 μg of protein extract was incubated overnight at 4 °C with the antibody of interest.

Culture and Treatment of Organotypic Cerebellar Slices. Cerebellar slices were cultured for 4 d as described previously (51). Slices were treated either with αFlk1 (30 μg/mL; ATCC), D-APV (25 μM), or a combination of αFlk1 plus D-APV by adding them to the culture medium.

Statistics. Unless specifically stated, data are expressed as mean ± SEM. Statistical analysis were performed by applying a paired Student's *t* test.

Please see *SI Materials and Methods* for detailed experimental procedures.

1. Ruiz de Almodovar C, Lambrechts D, Mazzone M, Carmeliet P (2009) Role and therapeutic potential of VEGF in the nervous system. *Physiol Rev* 89:607–648.
2. Ruiz de Almodovar C, et al. (2010) Matrix-binding vascular endothelial growth factor (VEGF) isoforms guide granule cell migration in the cerebellum via VEGF receptor Flk1. *J Neurosci* 30:15052–15066.
3. Lau CG, Zukin RS (2007) NMDA receptor trafficking in synaptic plasticity and neuropsychiatric disorders. *Nat Rev Neurosci* 8:413–426.
4. Newpher TM, Ehlers MD (2008) Glutamate receptor dynamics in dendritic microdomains. *Neuron* 58:472–497.
5. Papadia S, Hardingham GE (2007) The dichotomy of NMDA receptor signaling. *Neuroscientist* 13:572–579.
6. Luk KC, Sadikot AF (2004) Glutamate and regulation of proliferation in the developing mammalian telencephalon. *Dev Neurosci* 26:218–228.
7. Platel JC, et al. (2010) NMDA receptors activated by subventricular zone astrocytic glutamate are critical for neuroblast survival prior to entering a synaptic network. *Neuron* 65:859–872.
8. Lau PM, Zucker RS, Bentley D (1999) Induction of filopodia by direct local elevation of intracellular calcium ion concentration. *J Cell Biol* 145:1265–1275.
9. Zheng JQ, Wan JJ, Poo MM (1996) Essential role of filopodia in chemotropic turning of nerve growth cone induced by a glutamate gradient. *J Neurosci* 16:1140–1149.
10. Behar TN, et al. (1999) Glutamate acting at NMDA receptors stimulates embryonic cortical neuronal migration. *J Neurosci* 19:4449–4461.
11. Komuro H, Rakic P (1993) Modulation of neuronal migration by NMDA receptors. *Science* 260:95–97.
12. Mancini JD, Atchison WD (2007) The NR2B subunit in NMDA receptors is functionally important during cerebellar granule cell migration. *Neurosci Lett* 429:87–90.
13. Tárnok K, Czöndör K, Jelitai M, Czirók A, Schlett K (2008) NMDA receptor NR2B subunit over-expression increases cerebellar granule cell migratory activity. *J Neurochem* 104:818–829.
14. Dalva MB, et al. (2000) EphB receptors interact with NMDA receptors and regulate excitatory synapse formation. *Cell* 103:945–956.
15. Takasu MA, Dalva MB, Zigmond RE, Greenberg ME (2002) Modulation of NMDA receptor-dependent calcium influx and gene expression through EphB receptors. *Science* 295:491–495.
16. Chen BS, Roche KW (2009) Growth factor-dependent trafficking of cerebellar NMDA receptors via protein kinase B/Akt phosphorylation of NR2C. *Neuron* 62:471–478.
17. Cameron HA, McEwen BS, Gould E (1995) Regulation of adult neurogenesis by excitatory input and NMDA receptor activation in the dentate gyrus. *J Neurosci* 15:4687–4692.
18. d'Aldin CG, Ruel J, Assié R, Pujol R, Puel JL (1997) Implication of NMDA type glutamate receptors in neural regeneration and neoformation of synapses after excitotoxic injury in the guinea pig cochlea. *Int J Dev Neurosci* 15:619–629.
19. Watanabe M, Mishina M, Inoue Y (1994) Distinct spatiotemporal expressions of five NMDA receptor channel subunit mRNAs in the cerebellum. *J Comp Neurol* 343:513–519.
20. Rossi DJ, Slater NT (1993) The developmental onset of NMDA receptor-channel activity during neuronal migration. *Neuropharmacology* 32:1239–1248.
21. Hámori J, Somogyi J (1983) Differentiation of cerebellar mossy fiber synapses in the rat: A quantitative electron microscope study. *J Comp Neurol* 220:365–377.
22. Manzini MC, Ward MS, Zhang Q, Lieberman MD, Mason CA (2006) The stop signal revised: Immature cerebellar granule neurons in the external germinal layer arrest pontine mossy fiber growth. *J Neurosci* 26:6040–6051.
23. Losi G, Prybylowski K, Fu Z, Luo JH, Vicini S (2002) Silent synapses in developing cerebellar granule neurons. *J Neurophysiol* 87:1263–1270.
24. Kim BW, et al. (2008) Vascular endothelial growth factor (VEGF) signaling regulates hippocampal neurons by elevation of intracellular calcium and activation of calcium/calmodulin protein kinase II and mammalian target of rapamycin. *Cell Signal* 20:714–725.
25. Dawson NS, Zawieja DC, Wu MH, Granger HJ (2006) Signaling pathways mediating VEGF165-induced calcium transients and membrane depolarization in human endothelial cells. *FASEB J* 20:991–993.
26. Cheng HW, James AF, Foster RR, Hancox JC, Bates DO (2006) VEGF activates receptor-operated cation channels in human microvascular endothelial cells. *Arterioscler Thromb Vasc Biol* 26:1768–1776.
27. Faehling M, Koch ED, Raithel J, Trischler G, Waltenberger J (2001) Vascular endothelial growth factor-A activates Ca^{2+}-activated K$^+$ channels in human endothelial cells in culture. *Int J Biochem Cell Biol* 33:337–346.
28. Bocci G, et al. (2004) Increased plasma vascular endothelial growth factor (VEGF) as a surrogate marker for optimal therapeutic dosing of VEGF receptor-2 monoclonal antibodies. *Cancer Res* 64:6616–6625.
29. Farrant M, Feldmeyer D, Takahashi T, Cull-Candy SG (1994) NMDA-receptor channel diversity in the developing cerebellum. *Nature* 368:335–339.
30. Wang YT, Salter MW (1994) Regulation of NMDA receptors by tyrosine kinases and phosphatases. *Nature* 369:233–235.
31. Köhr G, Seeburg PH (1996) Subtype-specific regulation of recombinant NMDA receptor-channels by protein tyrosine kinases of the *src* family. *J Physiol* 492:445–452.
32. Salter MW, Kalia LV (2004) Src kinases: A hub for NMDA receptor regulation. *Nat Rev Neurosci* 5:317–328.
33. Zhang S, Edelmann L, Liu J, Crandall JE, Morabito MA (2008) Cdk5 regulates the phosphorylation of tyrosine 1472 NR2B and the surface expression of NMDA receptors. *J Neurosci* 28:415–424.
34. Olsson AK, Dimberg A, Kreuger J, Claesson-Welsh L (2006) VEGF receptor signalling - in control of vascular function. *Nat Rev Mol Cell Biol* 7:359–371.
35. Matsumoto T, et al. (2005) VEGF receptor-2 Y951 signaling and a role for the adapter molecule TSAd in tumor angiogenesis. *EMBO J* 24:2342–2353.
36. Courter DL, Lomas L, Scatena M, Giachelli CM (2005) Src kinase activity is required for integrin α$_V$β$_3$-mediated activation of nuclear factor-κB. *J Biol Chem* 280:12145–12151.
37. Mukhopadhyay D, et al. (1995) Hypoxic induction of human vascular endothelial growth factor expression through c-Src activation. *Nature* 375:577–581.
38. Wirkner K, et al. (2007) Modulation of NMDA receptor current in layer V pyramidal neurons of the rat prefrontal cortex by P2Y receptor activation. *Cereb Cortex* 17:621–631.
39. Chédotal A (2010) Should I stay or should I go? Becoming a granule cell. *Trends Neurosci* 33:163–172.
40. Gallo V, Ciotti MT, Coletti A, Aloisi F, Levi G (1982) Selective release of glutamate from cerebellar granule cells differentiating in culture. *Proc Natl Acad Sci USA* 79:7919–7923.
41. Eliceiri BP, et al. (1999) Selective requirement for Src kinases during VEGF-induced angiogenesis and vascular permeability. *Mol Cell* 4:915–924.
42. Zheng JQ, Poo MM (2007) Calcium signaling in neuronal motility. *Annu Rev Cell Dev Biol* 23:375–404.
43. Bjarnadottir M, et al. (2007) Neuregulin1 (NRG1) signaling through Fyn modulates NMDA receptor phosphorylation: Differential synaptic function in NRG1$^{+/-}$ knock-outs compared with wild-type mice. *J Neurosci* 27:4519–4529.
44. Oosthuyse B, et al. (2001) Deletion of the hypoxia-response element in the vascular endothelial growth factor promoter causes motor neuron degeneration. *Nat Genet* 28:131–138.
45. Yang SZ, Zhang LM, Huang YL, Sun FY (2003) Distribution of Flk-1 and Flt-1 receptors in neonatal and adult rat brains. *Anat Rec A Discov Mol Cell Evol Biol* 274:851–856.
46. Fulzele S, Pillai A (2009) Decreased VEGF mRNA expression in the dorsolateral prefrontal cortex of schizophrenia subjects. *Schizophr Res* 115:372–373.
47. Hardingham GE, Bading H (2010) Synaptic versus extrasynaptic NMDA receptor signalling: Implications for neurodegenerative disorders. *Nat Rev Neurosci* 11:682–696.
48. Stefansson H, Steinthorsdottir V, Thorgeirsson TE, Gulcher JR, Stefansson K (2004) Neuregulin 1 and schizophrenia. *Ann Med* 36:62–71.
49. Hatten ME (1985) Neuronal regulation of astroglial morphology and proliferation in vitro. *J Cell Biol* 100:384–396.
50. Salin PA, Malenka RC, Nicoll RA (1996) Cyclic AMP mediates a presynaptic form of LTP at cerebellar parallel fiber synapses. *Neuron* 16:797–803.
51. Renaud J, et al. (2008) Plexin-A2 and its ligand, Sema6A, control nucleus-centrosome coupling in migrating granule cells. *Nat Neurosci* 11:440–449.

NEUROSCIENCE